

# Barium titanate formation by organic resins formed with mixed citrate

J. P. COUTURES, P. ODIER

*Centre de Recherches sur la Physique des Hautes Températures, CNRS,  
45071 Orleans Cedex 2, France*

C. PROUST

*Laboratoire de Mécanique et Physique des Matériaux ESEM et CNRS-CRPHT,  
45071 Orleans Cedex 2, France*

Citric precursors are used to produce  $\text{BaTiO}_3$ , the Ba/Ti ratio being fixed by a mixed Ba–Ti citrate. The conditions for its solubility in organic agents (ethylene glycol or ethylene glycol + citric acid) has been studied and used to investigate various routes of synthesis (resin, spray pyrolysis or films). The transformation from the resin to the mineral phase has been investigated. In all cases the powders are aggregates of 150 nm. Their structure is cubic or tetragonal depending upon the route followed and they are at the limit of a structural metastability. Sintering may be accomplished below 1250 °C if the 150 nm aggregates are properly arranged. This depends upon the route chosen to produce them.

## 1. Introduction

The actual trend in the electronic ceramic industry is to develop a multilayer ceramic capacitor with the highest bulk capacity, thus the control of powder formulation is of crucial importance in this respect. Wet chemical methods are an area of intense research because of their inherent advantages compared to those of the more conventional solid state reaction processing.

The chemical synthesis of barium titanate has been recently reviewed by Phule and Risbud [1] and Chaput *et al.* [2]. A brief resumé of some of the ideas used by previous investigators is given in order to justify our approach.

A first attempt has been to realize a mixture of barium and titanium at the molecular level by producing, for example, co-hydrolysis of barium and titanium alkoxides. The major difficulty is to avoid the spontaneous self condensation between the Ti–OH groups leading to the formation of  $(-\text{Ti}-\text{O}-\text{Ti})_n$  clusters and a heterogeneous spatial repartition of barium and titanium. It provides, however, a significant advance with respect to the co-precipitation technique, but runs against the same final problem of chemical heterogeneity. The chemical modification of the alkoxides is now one way to overcome separate condensation [1, 3]. A more promising idea has been to force the reaction between the titanium complex  $\text{Ti}(\text{OH})_6^{2-}$  (in a strongly alkaline medium) and  $\text{Ba}^{2+}$  species to form directly the  $\text{BaTiO}_3$  in the solution. The detailed chemistry of this reaction is not yet known, but the possibility of hydrothermal-type reactions must be considered. Encouraging progress has been obtained: a cubic metastable phase of  $\text{BaTiO}_3$  has now been obtained at room temperature, but the

control of powder morphology is not yet so well resolved [2]. The hydrothermal route using  $\text{Ba}(\text{OH})_2$  is actually very promising for a low-temperature synthesis of microcrystalline  $\text{BaTiO}_3$  with control of the morphology. Another approach consists in the decomposition of double salts, such as oxalates, citrates and, more recently catecholates [4]. The implicit objective is to produce complex in which the titanium and barium ions have bonds and positions as close as possible to those in the barium titanate. However, the decomposition of these complexes is not simple and often passes through intermediates, possibly forming stable  $\text{BaCO}_3$  by decomposition. One of the advantages of this method is the precise reproducibility of the fixed Ba/Ti = 1 ratio.

One of the most successful routes using gelation techniques is the so-called liquid-mix technique [1, 5]. It is based on the formation of an organic–inorganic resin which contains the cations mixed homogeneously. There is a small segregation of the cations during the curing of the resin producing a barium titanate with a low sintering temperature [6].

The aim of this research was to combine the double-salt approach with that of the organic–inorganic resin. A good starting point seemed to choose the mixed citrate (MC)  $\text{BaTi}(\text{C}_6\text{H}_6\text{O}_7)_3 \cdot 6 \text{H}_2\text{O}$  [7, 8], which has the correct cationic stoichiometry and possibly a favourable arrangement of the barium and titanium. It was quickly apparent that this complex “soluble” in citric acid–ethylene glycol–water mixtures, i.e. a limpid mixture can be obtained, the detailed “structure” of which was not inferred. An attempt was made to obtain information about the parameters controlling the morphology of the powders obtained after thermal treatment. Therefore, several parameters were checked

and compared: decomposition of MC alone, of MC dissolved in citric acid–ethylene glycol–water mixtures in various proportions. This procedure is termed the “citric resin” process. Spray pyrolysis produced by an ultrasonic nebulizer was also tried as a means of modifying the internal packing of the particles. This provides a valuable way to evaluate the role of particle arrangement on the sintering of pure BaTiO<sub>3</sub>. Finally, thin layers were produced from a spray and their microstructure characterized.

## 2. Experimental procedure

### 2.1. Mixed Ba–Ti citrates

The preparation of mixed Ba–Ti citrate, i.e. BaTi(C<sub>6</sub>H<sub>6</sub>O<sub>7</sub>)<sub>3</sub>·6 H<sub>2</sub>O follows the procedure used previously [7, 8]. Barium chloride (BaCl<sub>2</sub>·2H<sub>2</sub>O, 99.5%) and Ti(OiPr)<sub>4</sub> (97%) were chosen as starting materials. A solution of complexed titanium was made first by adding Ti(OiPr)<sub>4</sub> to a 4 mol l<sup>-1</sup> solution of citric acid (CA), C<sub>6</sub>H<sub>8</sub>O<sub>7</sub>·H<sub>2</sub>O (99%) in demineralized water. A concentration of 1.12 mol Ti/l citric acid solution was used. The choice of the ratio CA/Ti(OiPr)<sub>4</sub> > 3 is appropriate to have a slight excess of citrate functions accounting for the stoichiometry of the MC. This mixture was heated, and at 80 °C, 1.12 mol Ba/l citric acid solution is added under stirring. During heating, isopropyl alcohol is released and the solution progressively clears. When the solution is clear and no further isopropyl alcohol is detected, it is cooled to room temperature during which time the mixed citrate precipitates. It is filtered and washed with water several times and recrystallized to purify it. The resulting compound is a white powder. The pH of the solution was adjusted below 2.6 in order to crystallize only BaTi(C<sub>6</sub>H<sub>6</sub>O<sub>7</sub>)<sub>3</sub>·6 H<sub>2</sub>O [7, 8].

### 2.2. Citric resin

The MC is easily dissolved in ethylene glycol (HO–CH<sub>2</sub>–CH<sub>2</sub>–OH) (EG) or in solutions of citric acid in this bifunctional alcohol. The resulting liquid is clear and perfectly stable with time, provided that the appropriate concentration of CA is respected. This point will be discussed in detail below. In certain cases,

heating may provide a means of achieving complete dissolution.

These solutions were polymerized at 150 °C forming a mixed organic-inorganic brownish resin containing immobilized barium and titanium cations. At this temperature, the elimination of water and ethylene glycol is detected by vapour phase chromatography. Upon reaching 250 °C, approximately 50% of the initial weight has been eliminated, the polymer is, therefore, a reticulated solid and is not soluble in water, ethanol or isopropyl alcohol. Several calcination procedures up to 700 °C at a rate of 50 °C h<sup>-1</sup> were used: flowing air or argon static air. Only the samples heated under flowing air were white; the others were grey due to an incomplete combustion of the carbon matrix.

### 2.3. Spray pyrolysis

In order to synthesize spherical shaped powders, the spray pyrolysis method at high temperature was used [9] in the 200–1000 °C range. It is especially suitable because the mixed citrate is soluble in ammoniacal aqueous solutions at pH ~ 6.3. This solution at a concentration of 2.3 × 10<sup>-2</sup> mol MC/l water can be sprayed by an ultrasonic piezoelectric transducer working at 2.5 MHz. The apparatus has been described previously [10]; it is schematically drawn in Fig. 1.

The spherical mist particles are introduced into a furnace having an adjustable temperature profile. They are collected in either an electrostatic-filter or on a sintered metallic filter. The residence time (1–10 s) is controlled by the gas carrier flow. The furnace fixes the maximum temperature, *T<sub>f</sub>*, experienced by the particles in this fast heating process.

### 2.4. Thin layers

Room-temperature spraying of MC solution in citric acid and ethylene glycol is possible, provided that the physical properties of the solution (viscosity, surface tension) are adequate. These parameters have not been measured. One composition based on the molar ratio 1 MC/47 CA/230 EG has been found to be successful in a preliminary test. This composition corresponds to a yield of 1 wt % BaTiO<sub>3</sub> after total reaction. The liquid is simply sprayed on an optically polished surface of various substrates (platinum, 3 mol % Y<sub>2</sub>O<sub>3</sub>-doped ZrO<sub>2</sub>, silica glass) and calcined at a heating rate of 50 °C h<sup>-1</sup> up to 700 °C, and maintained at this temperature for 4 h. Thin layers of BaTiO<sub>3</sub> were obtained.

### 2.5. Characterization

Several methods were used for characterizing the compounds: X-ray diffraction (XRD) (CuK<sub>α</sub> radiation), SEM, TEM, infrared and X-ray photoelectron spectroscopy. In addition specific surface areas were measured by nitrogen BET and the sintering behaviour by high-temperature dilatometry. Dry compacting

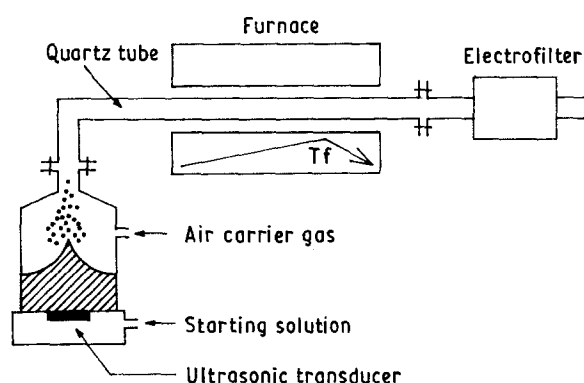


Figure 1 Spray pyrolysis apparatus.

was done in an isostatic press after vacuum pre-compactations in rubber fingers.

### 3. Results

#### 3.1. Mixed citrate

As assessed by Hutchins *et al.* [8] this mixed citrate process is very effective in defining the ratio Ba/Ti = 1 provided that the pH is fixed below 2.6, otherwise the compound  $\text{Ba}_2\text{Ti}(\text{C}_6\text{H}_5\text{O}_7)_2(\text{C}_6\text{H}_6\text{O}_7) \cdot x\text{H}_2\text{O}$  is obtained [7, 8]. This is a very fine and reproducible way to synthesize stoichiometric barium titanate, i.e. Ba/Ti = 1. This property has been used successfully in this study, as will be shown below.

The MC prepared by precipitation is a white crystalline powder obtained with a yield reaching 91%. The loss could come from a smaller titanium content in the solution than expected, due to the volatility of  $\text{Ti}(\text{OiPr})_4$  (b.p. 232 °C). The solubility of MC in hot water (90 °C) enables it to be purified by recrystallization. Even very large excesses of both cations, up to 12 mol %  $\text{BaCl}_2$  or 50 mol %  $\text{Ti}(\text{OiPr})_4$ , may be introduced into the mixture without any detectable perturbation in the crystallized compound. After calcination at 700 °C, the MC transforms into the pure barium titanate, free of polytitanate phases.

Very little is known about this compound. Its crystalline structure is not yet resolved although it is characterized only by its XRD powder pattern [8]. We have verified that it crystallizes with six water molecules by TGA. Its infrared spectrum (hexahydrated or monohydrated after heating at 160 °C) is very complex, Fig. 2 and Table I. It is insufficient to give a description of this molecule. However, based on these data and especially from the lines at 850, 625, 570  $\text{cm}^{-1}$ , the titanium is probably in an octahedral environment while a carboxyl group linked to a barium ion in a monodentate way is seen from the

vibrations at 1714 and 1297  $\text{cm}^{-1}$ . Owing to the lines at 3540 and 2570–2630  $\text{cm}^{-1}$ , free-acid functions  $\text{R}'\text{COOH}$  are expected, together with tertiary alcohol ROH for which the OH stretching vibration is probably at the origin of the line observed at 1575  $\text{cm}^{-1}$ . The observation of free-acid and tertiary alcohol functions in the MC are not surprising, owing to the  $\text{C}_6\text{H}_6\text{O}_7$  entities.

The thermal treatment of this precursor in air at 700 °C, for between 2 and 300 h gives a pure  $\text{BaTiO}_3$  phase having a tetragonal structure at ambient temperature. We note that the ratio  $c/a$  increases with the thermal treatment dwell time and reaches a value of 1.008 after 300 h ( $a = 0.4000$  nm and  $c = 0.4031$  nm). This evolution is not due to a variation in the size of the particles. These powders are constituted of aggregates of 150–200 nm, Fig. 3, themselves agglomerated into blocks. A de-agglomeration treatment is necessary to obtain low sintering temperatures.

#### 3.2. Citric resin

The existence of free acidic functional groups makes the mixed citrate soluble in CA–EG– $\text{H}_2\text{O}$  mixtures. We have studied, at room temperature, the CA–EG– $\text{H}_2\text{O}$ –1 mol MC isomolar cross-section of this quaternary diagram. In this section, the mixed citrate is represented by the point labelled MC in Fig. 4. Only the compositions lying in Zone 1 can give clear and stable solutions. For example, Point B

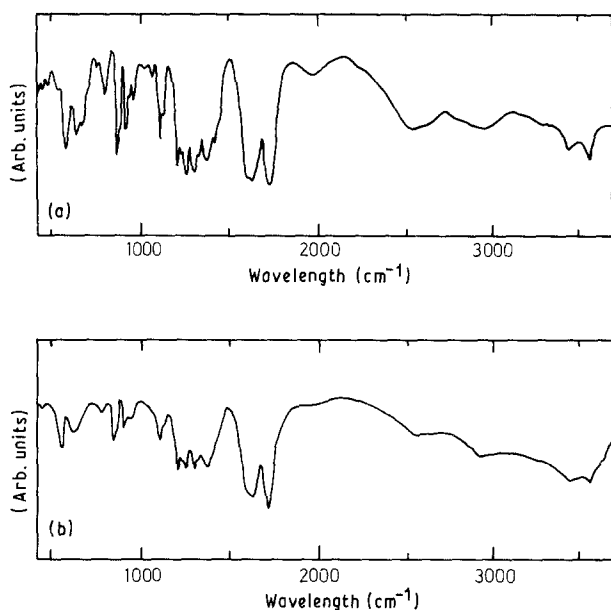


Figure 2 Infrared spectra of mixed citrates:

- (a)  $\text{BaTi}(\text{C}_6\text{H}_6\text{O}_7)_3 \cdot 6\text{H}_2\text{O}$ ,  
 (b)  $\text{BaTi}(\text{C}_6\text{H}_6\text{O}_7)_3 \cdot \text{H}_2\text{O}$ .

TABLE I Infrared data

Wavelength ( $\text{cm}^{-1}$ )	Vibration	
3617	Weak	Bending of O–H in $\text{H}_2\text{O}$ of crystallization
3540	Weak	Bending of O–H in free acid function
3426	Weak	
3270	Strong	
2800–3000	Large	Bending of C–H in $\text{CH}_2$
2570–2360	Strong	Bending O–H in a free acid function
1714	Large	Stretching asymmetry C–O in $\text{CH}_3\text{–COO–Ba}$ monodentate
1630	Weak	Water of crystallization
1575	Weak	Bending OH in tertiary alcohol
1297	Weak	Stretching symmetry in $\text{COO–Ba}$
853–625–570	Weak	Oxygen octahedral coordination of Ti

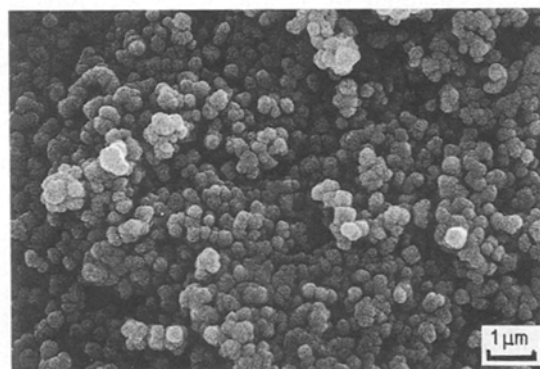


Figure 3 SEM on  $\text{BaTiO}_3$  from deagglomerated MC.

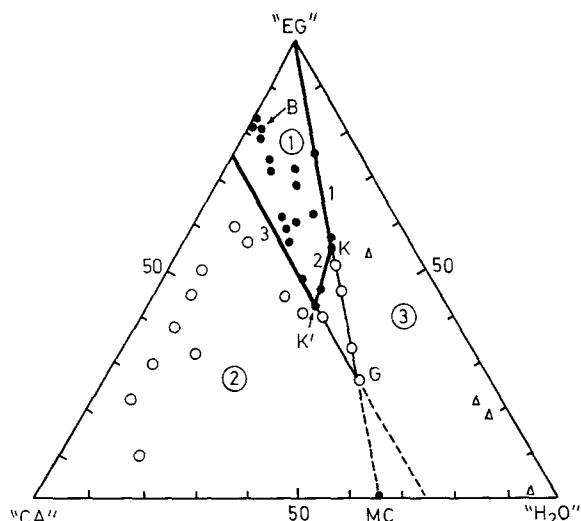


Figure 4 The CA-EG-H<sub>2</sub>O-1 mol MC isomolar cross-section. MC, G, K', K, B are points defined in the text. ● Clear solutions, (○) insoluble mixtures, (△) compositions giving clear solutions after heating. Lines 1, 2 and 3 delineated areas in which clear solutions of MC in CA-EG may be formed at room temperature.

(IMC/47CA/230EG) represents the composition used for the formation of thin layers of BaTiO<sub>3</sub> by the spray technique. The corresponding massive yield expressed by  $R = [\text{weight BaTiO}_3]/[\text{weight of the initial solution}]$  is 1% in this case. Compositions chosen in Zones 2 and 3 provide very viscous and white liquids or even wax. However, those located initially in Zone 3 can yield clear solutions after heating to 120 °C due to water evaporation.

We suppose that the dissolution of the mixed citrate occurs when ester and/or polyester functions are formed between free acidic functions of the MC and molecules of ethylene glycol. Indeed, ester functions have been identified by infrared spectroscopy in these citric resins [11]. In Fig. 4, Points ● represent compositions for which clear solutions can be formed. They are all in the area limited by lines 1-2-3. If one assumes three free acidic functions per MC molecule, which is reasonable in view of the formulae of the MC, one will need at least three EG and therefore 6 ROH functions per molecule of MC to form ester/polyester. Therefore, the EG could dissolve the MC up to a limit that is represented by Point K, on line 1 in Fig. 4. EG + CA should also be able to dissolve MC, provided the ratio of alcoholic ROH functions/acidic R'COOH functions, in the solvent, is larger than 2. Line 3 is defined as a line corresponding to a ratio  $\text{ROH}/\text{R}'\text{COOH} = 2$ . Along this border one can increase the MC content until Point K' is reached, above which no clear solution is formed. This defines a new limit K-K', labelled 2, Fig. 4. This line corresponds to a ratio  $N_{\text{H}_2\text{O}}/(\text{F}_{\text{ROH}} + \text{F}_{\text{R}'\text{COOH}}) < 1/3$ , where  $N_{\text{H}_2\text{O}}$  represents the number of water molecules,  $\text{F}_{\text{ROH}}$  the number of alcoholic functions brought by the EG and  $\text{F}_{\text{R}'\text{COOH}}$  the number of acidic functions, i.e. the free acidic functions from the MC plus those from the CA. Line 2 appears to correspond, in fact, to the limit of the esterification reaction at room temperature. This qualitative approach enables one to predict the range in which such a liquid resin process can be developed.

Upon heating in static air, this mixed organic-inorganic resin transforms until complete mineralization has occurred. Owing to the essential role played by EG, its elimination by heating (around 250 °C) leaves a resin completely insoluble in most alcohols. The first traces of a mineral phase are observed at 350 °C. At this temperature the sample appears to be composed of a white, a white plus grey, and a grey part, due to a departure from the equilibrium conditions in the non-circulated furnace. The black part resulted from the partial decomposition of the precursor in an unidentified graphitic phase plus an amorphous phase while the white part is composed of BaCO<sub>3</sub> and BaTiO<sub>3</sub> traces, Fig. 5. The plots of infrared spectra versus temperature, Fig. 6, show that the BaCO<sub>3</sub> phase (detected with a great sensitivity due to the intense  $\nu_3$  band at 1460 cm<sup>-1</sup>) grows at the expense of ester functions of the resin and probably barium itaconates [7] found together in the complex band at 1500-1850 cm<sup>-1</sup>. Calcination under circulated argon leads to different results. Firstly, the temperature of onset of mineralization is much higher (700 °C) than in air. Secondly, if the decomposition of the resin also gives graphitic phases, no BaCO<sub>3</sub> is detected simultaneously with the crystallization of BaTiO<sub>3</sub>. This tends to show that under argon the cationic chemical homogeneity of the resin is preserved. On the contrary, when the oxygen potential is too high (flowing air), an exothermic combustion of the resin occurs which destroys, locally the precursor. Effectively, one observes hot spots in the powder

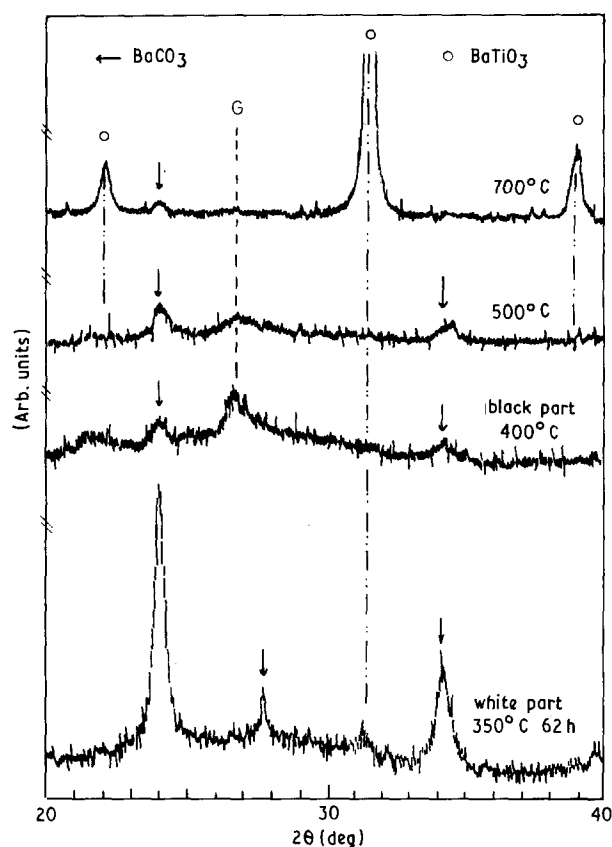


Figure 5 XRD of powders from citric resin B (1%) versus calcination temperature in air.

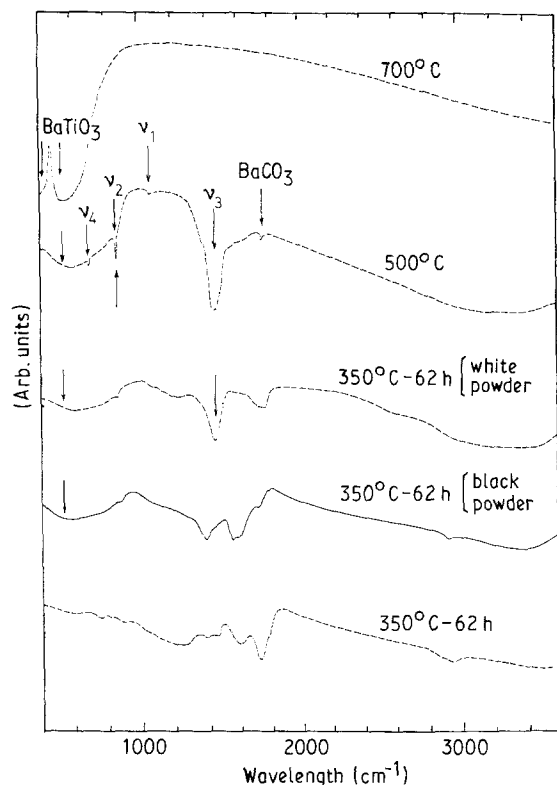


Figure 6 Infrared spectra of powders from citric resin B (1%) versus calcination temperature in air.

during the thermal treatment that have also been seen by infrared thermography during the synthesis of  $\text{MgTiO}_3$  by air decomposition of (Mg, Ti) propionic resin [12]. This collapse of the precursor probably sets aside relatively free barium immediately carbonated and  $\text{TiO}_2$  not detected by XRD. This effect is, however, probably rather local, otherwise the amount of  $\text{TiO}_2$  should be greater than so far detected by XRD. In this case, a higher temperature treatment would be necessary to accomplish the recombination reaction between  $\text{BaCO}_3$  and  $\text{TiO}_2$ . In summary, in agreement with Mulder [13], we believe that under appropriate oxygen potential conditions, the high chemical homogeneity of the precursor may be retained during its decomposition, leading to the obtention of  $\text{BaTiO}_3$  at a moderate temperature. At the end of the reaction ( $700^\circ\text{C}$  in static air) a pure  $\text{BaTiO}_3$  phase is obtained, free of  $\text{BaCO}_3$  as detected by infrared spectroscopy, and its crystalline form is cubic at room temperature. Annealing at  $700^\circ\text{C}$ , for long times (up to 300 h), does not produce any significant evolution of their structure, contrary to the previous case of those produced from the MC.

The microstructure is one of the aspects which it is necessary to monitor during the production of the powder. In the present case, one can distinguish three ranges (Fig. 7): (1) micro-crystallites ranging from 25–80 nm in a platelet shape, (2) crystallites associated into 150 nm spheroidic aggregates, (3) these aggregates linked in wider agglomerates the shape and size of which are related to the massive yield already defined above. For low mineral content, i.e.  $R < 4\%$ , one observes plate-like agglomerates in which the spheroid particles are regularly distributed. Irregular

and porous blocks are formed for richer mineral contents. They are larger and more compact for higher  $R$ . These differences induce in a complex way a memory effect of the powder's thermal history (exothermic reactions giving rise to more or less strong agglomerates), combined with the influence of the physical properties of the resins (viscosity, surface tension). One can justify the weaker agglomerated structure of the powders produced from diluted resins ( $R = 1\%$ ) by the larger volume eliminated before the exothermic combustion of the polymer.

These powders have a high sinterability after a suitable de-agglomeration which can be done by ultrasonic dispersion. The sintering, at constant heating rate, ends below  $1250^\circ\text{C}$  with a density approaching 99% theoretical, Fig. 8, Curve 1a. Curve 1b is the first derivative of the shrinkage versus  $T$ . The shrinkage rate versus  $T$  shows a maximum at  $1060^\circ\text{C}$  which is assumed to correspond to the elimination of the porosity due to the packing of the 150 nm particles.

### 3.3. Spray pyrolysis

The spray pyrolysis method is very interesting as a fine tool to produce spherically shaped powders [9–11, 14, 15], but here they are hollow spheres as it will be shown later. Several remarks can be made which may be profitable in the understanding of the process using the MC.

1. The spray pyrolysis is a fast firing process, and obviously in the present case, the as-collected powders have not reached their equilibrium state. They should be in a state similar to those picked up in the transient stage  $300\text{--}500^\circ\text{C}$ , described above. Indeed the particles collected at  $T_f = 900^\circ\text{C}$  show the initiation of the crystallized  $\text{BaTiO}_3$  phase plus an unidentified graphitic phase with no barium carbonate, Fig. 9. This is very similar to the product obtained from the citric resin route under argon or at  $350^\circ\text{C}$  in air. The annealing of this powder at  $400^\circ\text{C}$  in air burns the graphite phase with a simultaneous increase in the specific surface area of the powders and the formation of barium carbonate. The graphite was therefore present as a sealing cement. Further annealing at  $700^\circ\text{C}$  provides the pure  $\text{BaTiO}_3$  cubic phase.

2. During the annealing, the burning out of the carbon phase reveals the hollow microstructure of these spheres (Fig. 10). The powder annealed at  $700^\circ\text{C}$  is composed of 150–200 nm particles agglomerated together. These small entities are similar to those obtained from the citric resin process.

3. It is interesting to compare the sintering of this powder with that of de-agglomerated powders from the citric resin process. Both have similar building units but are packed in a very different way. The sintering behaviour is interesting to compare. It ends up only above  $1300^\circ\text{C}$  (Fig. 8, curve 2a), the derived shrinkage versus  $T$  curve (Fig. 8, curve 2b) shows an extremum at  $1060^\circ\text{C}$  corresponding to the sintering of the 150 nm aggregates, as in the powders from the citric resin. The temperature must be raised to more than  $200^\circ\text{C}$  above this before the voids of these hollow

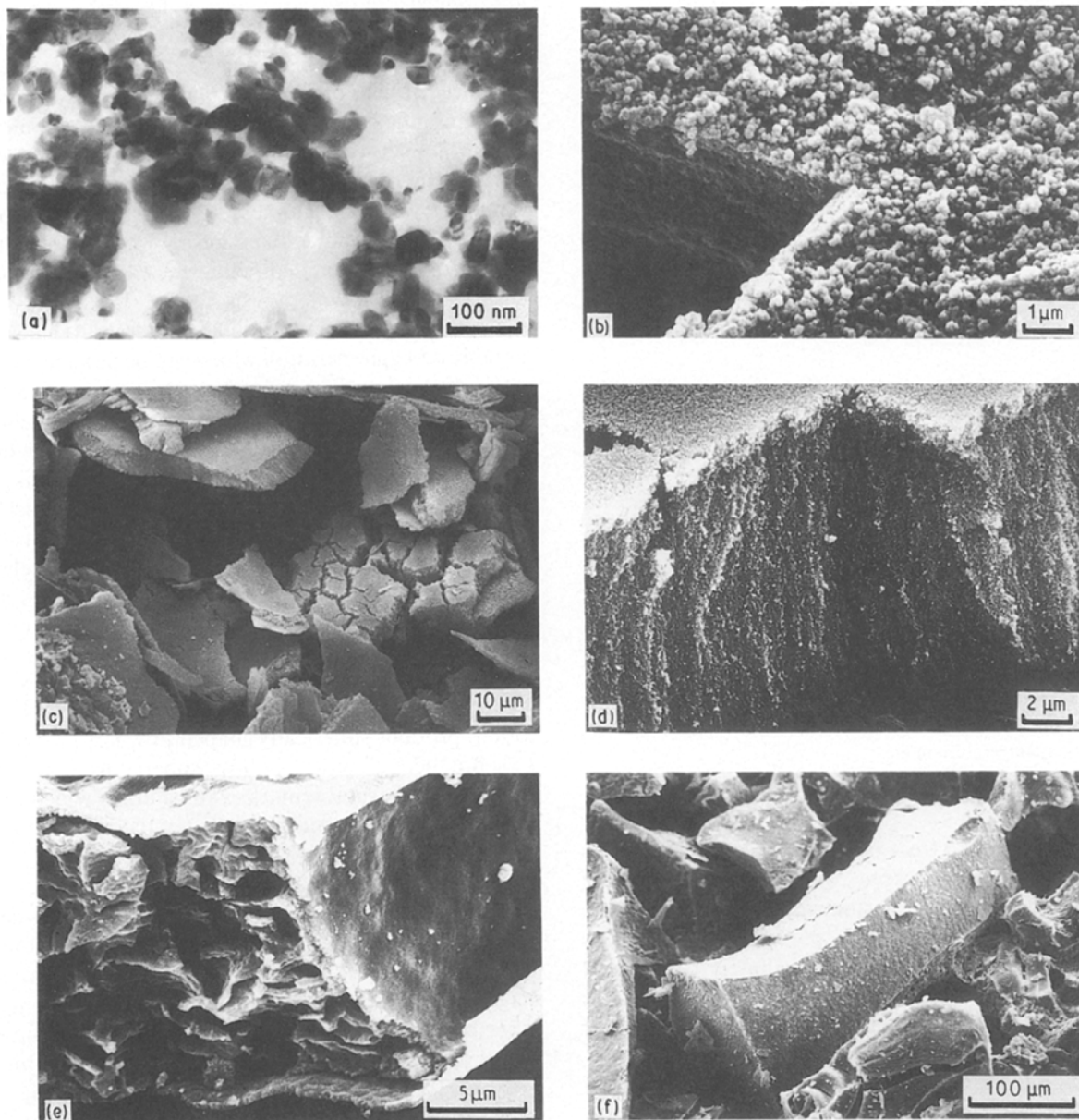


Figure 7 Relation between the morphology and the dilution of the precursor (massive yield), (a) by TEM on ultra-thin sections (this building unit of the powder ranges between 20 and 80 nm); (b-d) by SEM on diluted resins  $R = 1\%$  photos; (e, f) for increasing inorganic ratio, (e)  $R = 8\%$ , (f)  $R = 11\%$ .

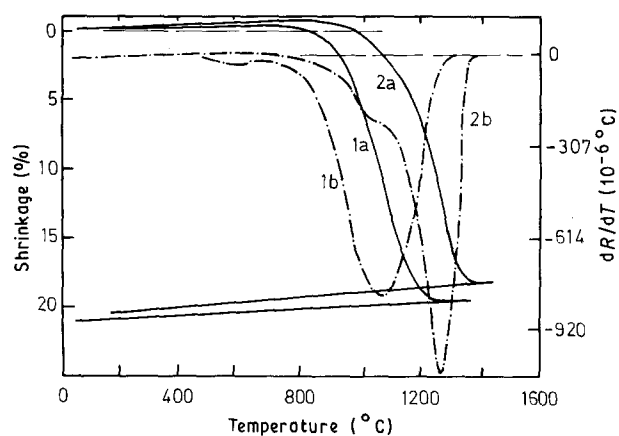


Figure 8 Sintering of (1a) deagglomerated powders produced from citric resin  $R = 1\%$  (heating rate  $300^\circ\text{C h}^{-1}$ ), (1b) powder from spray-pyrolysed MC further annealed at  $700^\circ\text{C}$  in air. (---) The derivative over  $T$  of the shrinkage (right scale).

spheres are eliminated. This emphasizes once more the role of packing on sintering [16].

### 3.4. Thin layers

The best results have been obtained on polished silica glasses for diluted citric resins ( $R = 1\%$ ). In proper conditions a continuous thin layer is formed after calcination at  $700^\circ\text{C}$ , it is free of defects over several square millimetres, Fig. 11a. Flaws are probably formed on uncontrolled dust (Fig. 11b). The layer is constituted of  $\text{BaTiO}_3$  and has been characterized by SEM, infrared and XPS. Its thickness has been evaluated by SEM to be about 200 nm, in very good agreement with the estimation obtained by the attenuation of the infrared transmitted signal. XPS yields evidence that the layer is free of silicon; this confirms first its continuity and secondly proves a low diffusion of silicon

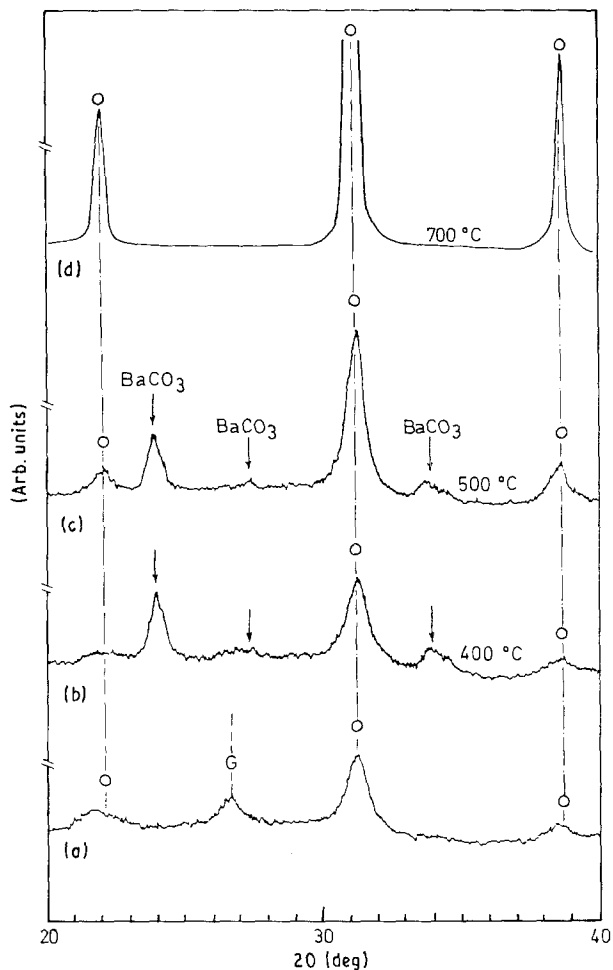


Figure 9 XRD diagrams of powders from spray-pyrolysed MC in ammoniacal aqueous solution at 900°C, (a) as-collected, (b) annealed at 400°C, (c) annealed at 500°C, (d) annealed at 700°C, G, graphite; O, BaTiO<sub>3</sub>.

from the substrate toward the surface of the BaTiO<sub>3</sub> layer. A few per cent of BaCO<sub>3</sub> is detected at the surface, it is expected to come from atmospheric contamination of the sample before the XPS measurement.

#### 4. Discussion

One of the interesting aspects of the results presented above concerns the morphology of the particles produced by these four processes. They are composed of micro-crystalline primary particles (platelets) associated in spheroidal aggregates the sizes of which are remarkably independent of the method used to produce them. Morphology is therefore suspected to depend mainly on the MC properties. The relationship between the precursor properties and the morphology of the resulting powders is one of the things which must be worked out in the future.

The exploration of particle-size effects on physical properties is a very interesting and newly opened field, owing to the accessibility of nanometric particles. It is now well documented in the ferroelastic zirconia that small particle sizes can significantly decrease the martensitic temperature [17–19] up to 500°C. Similar effects are also known in bulky ferroelectric materials [20]: in sufficiently small-grained ceramics, the stress reduction by twinning cannot lower the total energy,

the grains then remain in a metastable state. Recently, size effects on the ferroelectric phase transition of PbTiO<sub>3</sub> [21] and BaTiO<sub>3</sub> [22] have been reported in ultrafine particle powders. In the latter case a critical size of 120 nm has been found below which the compound remains in its high-temperature cubic phase. The powders produced from the citric routes appear to behave similarly. Their sizes are in the range 150–120 nm, at the border of the critical size. It is thus suspected that small surface energy modifications or residual stresses could shift the critical size to a slightly higher value. Such differences could exist between the powders resulting from the MC and the citric resin processes. This could explain why the powders from the MC process become tetragonal after annealing, while those from the citric resin remain cubic at room temperature.

#### 5. Conclusion

The formation of barium titanate by using a mixed citrate precursor has been studied. The mixed citrate is

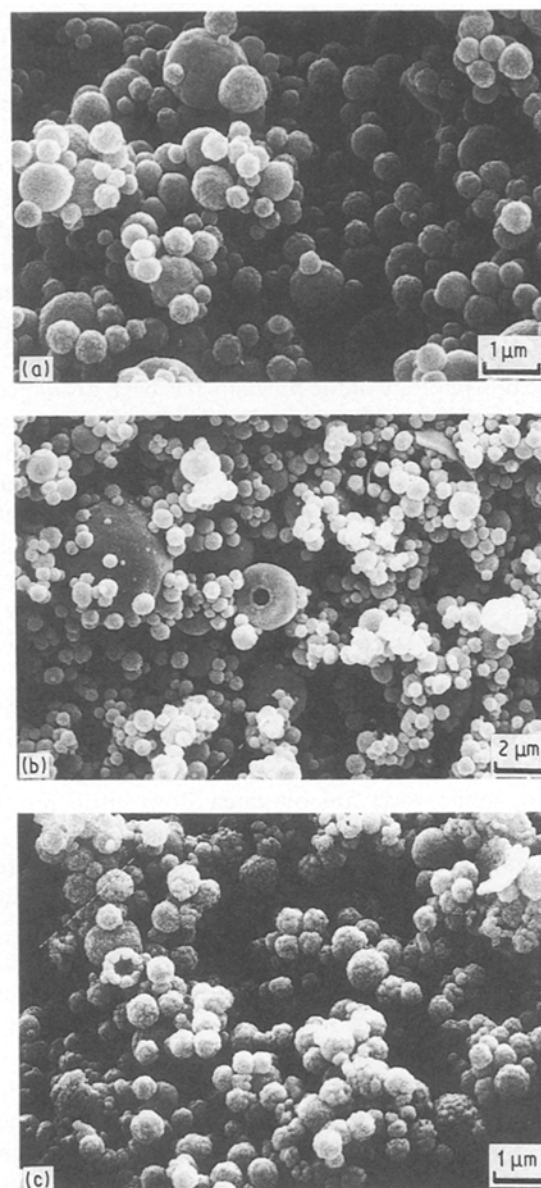


Figure 10 SEM of powders obtained by spray pyrolysis of MC in ammoniacal aqueous solution, (a) as-collected, (b) annealed at 400°C, (c) annealed at 700°C.



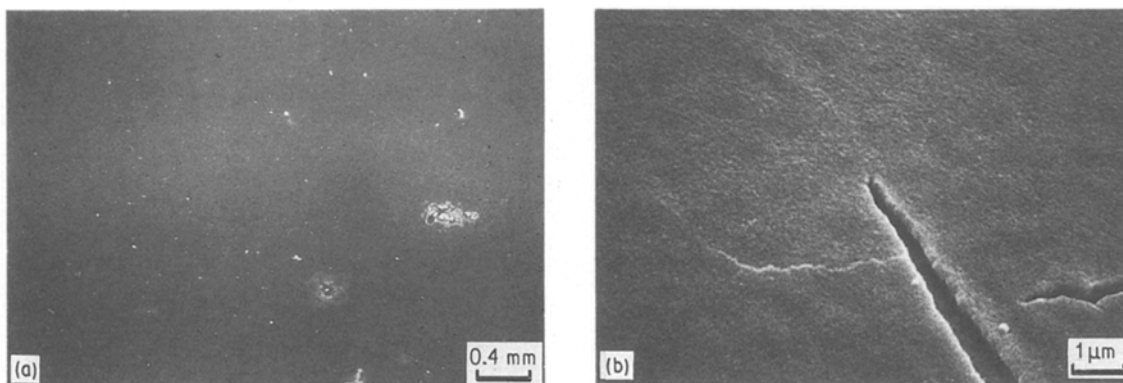


Figure 11 (a, b) A thin layer of BaTiO<sub>3</sub> (200 nm thick) obtained by spraying a liquid citric precursor (composition labelled B in the text) on silica glass at room temperature and calcining it at 700 °C.

an interesting way to prepare reproducibly stoichiometric barium titanate. This compound can be used alone or in solution in a multifunctional alcohol such as ethylene glycol. Although not entirely elucidated the mechanism of solubility lies in the existence of free acidic functions of the MC-producing soluble esters.

The thermal treatment of the pure or diluted MC involves the decomposition of organic groups by a complex mechanism; the oxygen activity value in the gas phase is therefore of prime importance. The present work suggests that the decomposition may proceed without destruction of the chemical homogeneity if excessive exothermic combustion can be avoided. Even when this is not the case, in conventional air treatment, the transformation ends with a solid state reaction at 700 °C which concerns only a small part of the sample.

The morphology of the powders has been examined under four experimental conditions described above (transformation of the MC, transformation of the citric resin, spray pyrolysis and thin layers). Several levels should be distinguished. At the lower level, individual micro-crystals are formed which range in size between 20 and 80 nm. They are the primary particles, are associated in spheroidal 150 nm aggregates and their size appears to be remarkably independent of the experimental conditions.

The sinterability of the powders produced from the MC process is excellent, provided they are properly de-agglomerated. The best results (sintering at 1250 °C in a dynamic way) are obtained from citric resins ultrasonically de-agglomerated. On the contrary, powders obtained from spray pyrolysis, which are made of the same entities, but arranged in hollow spheres, sinter at higher temperatures.

Thin continuous layers of BaTiO<sub>3</sub> have been obtained by simply spraying an adequate solution of MC. This is a rather simple way to produce ferroelectric films.

Finally, the structure of all these powders is at the limit of a critical size favouring stabilization of the high-temperature cubic phase. Just a small variation in the process, i.e. MC decomposition or citric resin, may modify the structure to the stable or metastable state. More work is necessary to understand the origin of such differences.

## Acknowledgements

This work was supported financially by the Regional Council "Région Centre" and CNRS. We thank Dr A. Douy for many enlightening discussions, Dr R. Erre for the XPS characterization, Dr F. Gervais for the infrared characterization, and P. Canale for technical assistance.

## References

1. P. P. PHULE and S. H. RISBUD, *J. Mater. Sci.* **25** (1990) 1169.
2. F. CHAPUT, J. P. BOILOT and A. BEAUGER, *J. Amer. Ceram. Soc.* **73** (1990) 942.
3. J. LIVAGE, M. HENRY and C. SANCHEZ, *Progr. Solid State Chem.* (18) (1989) 259.
4. J. A. DAVIES and S. DUTREMEZ, *J. Amer. Ceram. Soc.* **73** (1990) 1429.
5. P. A. LESSING, *Amer. Ceram. Bull.* **68** (1989) 1002.
6. H. SALZE, P. ODIER and B. CALES, *J. Non Cryst. Solids* **82** (1986) 314.
7. D. HENNINGS and W. MAYR, *J. Solid State Chem.* **26** (1976) 329.
8. G. A. HUTCHINS, G. H. MAHER and S. D. ROSS, *Amer. Ceram. Bull.* **66** (1987) 681.
9. B. DUBOIS, D. RUFFIER and P. ODIER, *J. Amer. Ceram. Soc.* **72** (1989) 113.
10. P. ODIER, B. DUBOIS, C. CLINARD, H. STROUMBOS and Ph. MONOD, in "Ceramic Powders Science III" Ceramic Transaction Vol. 12, edited by G. L. Messing, Shin-ichi Hinano, and H. Hausen (The American Ceramic Society, Westerville, OH, 1990) p. 75.
11. C. PROUST, Thèse de Doctorat de l'université d'Orléans (1990).
12. M. JOURDAN, Thèse de Doctorat de l'université de Bourgogne (1987).
13. B. J. MULDER, *Amer. Ceram. Bull.* **49** (1970) 990.
14. H. ISHIZAWA, O. SAKURAI, N. MIZUTANI and M. KATO, *J. Amer. Ceram. Soc.* **65** (1986) 1399.
15. Y. KANNO and T. SUZUKI, *J. Mater. Sci. Lett.* **7** (1988) 386.
16. F. F. LANGE, *J. Amer. Ceram. Soc.* **72** (1989) 3.
17. C. A. ANDERSSON, J. GREGGI and T. K. GUPTA, in "Advanced Ceramics", Vol 3, edited by A. H. Heuer and L. W. Hobbs (The American Ceramic Society, Columbus, OH, 1981) p. 184.
18. R. C. GARVIE and M. F. GOSS, *J. Mater. Sci.* **21** (1986) 1253.
19. B. BASTIDE, P. CANALE and P. ODIER, *J. Eur. Ceram. Soc.* **5** (1989) 289.
20. G. ARLT, *J. Mater. Sci.* **25** (1990) 2655.
21. K. ISHIKAWA, K. YOSHIKAWA and N. OKADA, *Phys. Rev. B* **37** (1988) 5852.
22. K. UCHINO, E. SADANAGA and T. HIROSE, *J. Amer. Ceram. Soc.* **72** (1989) 1555.

Received 28 November 1990  
and accepted 18 March 1991